

PACS numbers: 41.75.Jv; 41.75.Ak; 73.63.–b
DOI: 10.1070/QE2012v042n01ABEH014607

Optimal acceleration of ions by laser pulses with a sharp leading edge*

V.V. Kulagin, V.N. Kornienko, V.A. Cherepenin, H. Suk

Abstract. **We consider acceleration of ions through the interaction of a laser pulse with a sharp leading edge with nanofilms. At sufficiently large amplitude of the pulse, all the electrons can be expelled from the film, which provides an effective regime of ion acceleration. Limiting the maximum energy of ions can result from the longitudinal reverse motion of electrons to the initial position and by the transverse motion of electrons along the nanofilm surface, which causes the ion charge compensation. The characteristic parameters of the dynamics of ions and electrons in the system are analytically evaluated, which agree well with the results of two-dimensional numerical simulations by the particle-in-cell method. Optimisation of the acceleration process by using the analytical estimates makes it possible to select the optimal parameters of the laser pulse and nanofilm. Numerical simulation of ion acceleration at these parameters shows that the maximum energy of ions can be substantially increased.**

Keywords: *laser acceleration of ions, ultra-high-power laser pulses with an extremely sharp leading edge, relativistic electron mirrors.*

1. Introduction

In the past decade, laser acceleration of ions has attracted much attention. Many papers are devoted to the study of different regimes of acceleration by linearly polarised [1–17] and circularly polarised [18–29] pulsed laser radiation, which opens up new vistas to use laser-accelerated ions, for example, in radiography of transients processes, in hadron therapy of cancer, in isochoric target heating, etc.

Among the theoretical papers on ion acceleration by linearly polarised pulsed lasers, many publications are devoted to the study of different acceleration mechanisms. Such mechanisms involve acceleration of ions by a fast electron cloud emission from the target [3, 5, 6, 14–16] (target normal sheath acceleration, TNSA), typical of thick targets; ion acceleration by radiation pressure [8]; acceleration in the directed-Coulomb-explosion regime [9, 13]; and combined variants when several mechanisms of acceleration alternate during the interaction of a laser pulse with the target [11–13]. In many acceleration schemes, the laser pulse power and energy must be extremely high (see, for example, [8]), which hinders the use of these schemes at present.

The theory of the TNSA mechanism is sufficiently well developed (see, for example, [3, 6, 14, 15]). However, the characteristics of ion beams formed by such acceleration are unsatisfactory for many applications. Numerical simulation shows that significantly better results at a relatively low power of the laser system (no more than several petawatts) can be achieved for the acceleration of ions by the Coulomb explosion or by the use of different combined variants [9, 11–13]. Theoretical description here is more complicated, because the adiabatic approximation used to describe the electron distribution function is not applicable. Therefore, the development of theory and optimisation methods of ion acceleration by laser pulses with an extremely sharp leading edge and a moderate energy is crucial for effective implementation of the process.

The purpose of this paper is to investigate the physical mechanisms that limit the maximum energy of the ions during their acceleration by laser pulses with an extremely sharp leading edge, and to develop an analytical approach that makes it possible to optimise the acceleration process. The ions will be accelerated most effectively when the electrons are completely expelled from the nanofilm. It is this case that is realised in the generation of relativistic electron mirrors [30, 31]. Indeed, if the longitudinal component of the Lorentz force is larger than the Coulomb force of attraction between the ions and electrons, all the electrons of the nanofilm move synchronously in the direction of the laser pulse propagation and are expelled from the nanofilm. After some time, called the lifetime of a relativistic electron mirror, the electrons begin to turn back, and the first to turn back are the electrons that are affected by the maximum Coulomb force; at the same time, some electrons continue to move in the same direction. To generate relativistic electron mirrors, there was developed a self-consistent analytical theory of acceleration, which takes into account the collective radiation of electrons, depletion of the laser pulse passing through the nanofilm and the Coulomb forces and allows one to estimate the lifetime of a relativistic electron mirror and its other parameters [30, 31].

When generating relativistic electron mirrors, the most efficient is the use of laser pulses with an extremely sharp leading edge, where even the first half-cycle has an amplitude

*Reported at the Conference 'Laser Optics', Russia, St. Petersburg, June 2010.

V.V. Kulagin Sternberg Astronomical Institute, M.V. Lomonosov Moscow State University, Universitetskii prosp. 13, 119992 Moscow, Russia; e-mail for correspondence: victorvkulagin@yandex.ru;
V.N. Kornienko, V.A. Cherepenin Institute of Radio Engineering and Electronics, Russian Academy of Sciences, ul. Mokhovaya 11, 125009 Moscow, Russia;
Hyyong Suk Advanced Photonics Research Institute, Gwangju Institute of Science and Technology, 261 Cheomdan-Gwagiro (Oryong-Dong), Buk-gu, Gwangju 500-712, Republic of Korea; e-mail for correspondence: hysuk@gist.ac.kr

Received 25 February 2011; revision received 21 September 2011
Kvantovaya Elektronika **42** (1) 58–64 (2012)
Translated by I.A. Ulitkin

close to the maximum amplitude of the pulse (non-adiabatic pulses). In this case, to minimise the energy, use should be made of few-cycle pulses (two-to-three optical cycle pulses). 4.5–5-fs pulses at multigigawatt powers were experimentally obtained some time ago [32]; higher-power pulses with a power of about ten terawatt and a duration of 8.5 fs or less were generated in [33]. For petawatt pulses with an energy of tens of joules, possible schemes of generation (shaping) are considered [34, 35]. At the same time, numerical simulation shows that the leading edge steepness is more important for generation of relativistic electron mirrors than for ion acceleration; here, much more important is the energy and the maximum amplitude of the laser pulse. Below, we will use in numerical simulations laser pulses with a power of 1–2 PW and a duration of three periods of the laser field (and with a sharp edge). In this case, the pulse energy is less than 20 J.

2. Two-dimensional numerical simulation of ion acceleration by laser pulses with a sharp leading edge

In two-dimensional simulations we used the XOOPIC code [36]. To accelerate the ions, use was made of a linearly polarised laser pulse propagating in the positive direction of the x axis. The wavelength of laser light in vacuum was $\lambda = 1$ μm, the dimensionless field amplitude was $a_0 = |e|E_0/(mc\omega) = 12-40$, where c is the speed of light in vacuum; ω and E_0 are the frequency and amplitude of the laser field in vacuum; e and m are the electron charge and mass. In the transverse direction, the laser pulse had a Gaussian profile with a radius of the beam waist $w_0 = 8\lambda$ (at the e^{-1} level). Duration of the rectangular pulse envelope in the longitudinal direction was three periods of the laser field. The thickness of the nanofilm was $l = 10$ nm, the normalised surface charge density of the nanofilm was $\alpha = \pi(\omega_p^2/\omega^2)(l/\lambda) = 3$ [$\omega_p = (4\pi n_0 e^2/m)^{1/2}$ is the plasma frequency, and n_0 is the electron density of a nanofilm], which corresponds to $n_0 = 95.5n_{cr}$, where n_{cr} is the critical electron density for $\lambda = 1$ μm. We assumed that the atoms of the nanofilm were completely ionised (estimates show that for the field amplitudes used in the simulations, this assumption holds true), and the plasma was collisionless. When modelling the acceleration, the ion mass was $m_i = 1840m$.

The time dependence of the maximum energy of accelerated ions near the laser beam axis in the case of a nanofilm with $\alpha = 3$ is shown in Fig. 1 for $a_0 = 18$ (see also Fig. 5 for $a_0 = 30$; the time is measured from the beginning of interaction). Similar curves for other system parameters are given in [17]. First, the ion energy increases as if the acceleration occurs in a constant field (solid curve in Fig. 1). This means that all the electrons are expelled from the nanofilm by a laser pulse. The ions with a maximum energy are located between a layer of other ions and a layer of electrons, i.e., they are accelerated as if in a field of a plane capacitor. In this case, the longitudinal accelerating field is the sum of the fields generated by ions and electrons, and the ion energy ε increases with time according to the law (hereafter in formulas the time $\tilde{t}$ is normalised to the period T_0 of the laser field):

$$\varepsilon = \left[\sqrt{1 + (2\zeta\tilde{t})^2} - 1\right]\varepsilon_{0i} \simeq 2\varepsilon_{0i}(\zeta\tilde{t})^2, \qquad (1)$$

where

$$\zeta = \frac{2\pi\alpha m}{M}; \qquad (2)$$

ε_{0i} and M are the rest energy and the ion mass. It follows from expression (1) that the maximum ion energy is four times higher than the ion energy during acceleration in the field of the positively charged plane with the same surface charge. In addition, this field distribution results in a strongly asymmetric expansion of the ions, directed mainly to the same side, where the laser light propagates (see Figs 2 and 3 below). These features provide a high rate of acceleration at which the duration of the effective acceleration interval is no more than 10–20 periods of the laser field (see Fig. 7 and its discussion), and the electrons do not have time to get far away from their initial position.

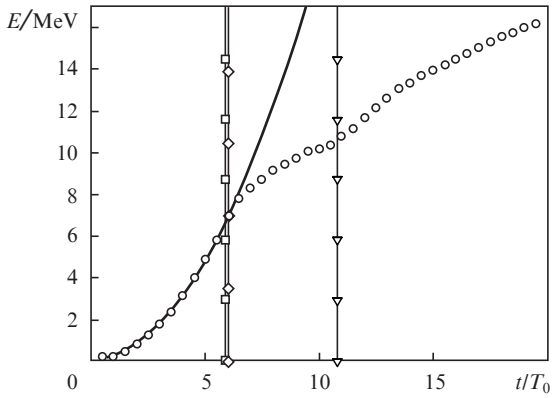

Figure 1. Time dependence of the maximum energy of the nanofilm ions (protons) in the vicinity of the laser beam axis for $a_0 = 18$ and $\alpha = 3$ (curve with circles). The solid curve corresponds to the energy of the ions during their acceleration in a constant field. The vertical lines show the characteristic times during acceleration of the ions.

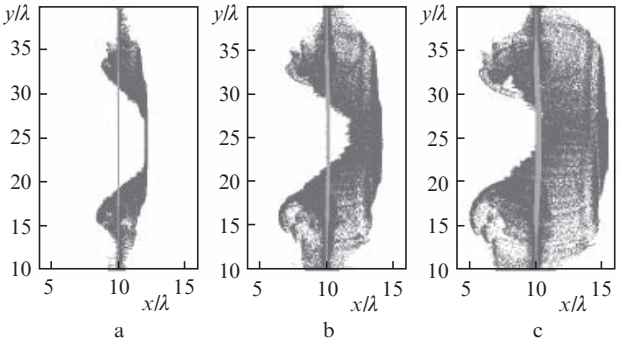

Figure 2. Phase spaces x, y of the electrons (dark grey areas) and the ions (light grey areas) at $t = 2.5T_0$ (a), $4.5T_0$ (b) and $5.9T_0$ (c) from the beginning of interaction for $\alpha = 3$. Acceleration is implemented by a laser pulse with the normalised field amplitude $a_0 = 18$ and the waist radius $w_0 = 8$.

The accelerating curve (Fig. 1) has a point at which the growth of acceleration rate starts decreasing, and the acceleration curve deviates from the theoretical dependence for the acceleration in a constant field. This point can be naturally called the effective time of the ion acceleration t_{ea}. First, t_{ea} increases with field amplitude (see Fig. 1 and Fig. 5 below). However, with increasing amplitude from 30 to 40 (for $\alpha = 3$)

the time of effective acceleration remains virtually the same. Thus, there are two physical processes that, firstly, result in the presence of an inflection point at the acceleration curve, and, secondly, limit the duration of effective acceleration with increasing field amplitude. Both mechanisms will be studied in detail below.

3. Time of effective acceleration of ions by laser pulses with an extremely sharp edge

3.1. Limiting the maximum energy of the ions due to the longitudinal return of electrons to the initial position

Characteristics of evolution of a relativistic electron mirror are studied in detail in [30, 31]. The phase spaces x, y of the electrons and ions for the nanofilm with $\alpha = 3$ are shown in Fig. 2 at different times from the beginning of interaction (see also [17]). Acceleration is implemented by a laser pulse with $a_0 = 18$. At $t = 2.5T_0$, the relativistic mirror is not yet damaged and is located at point $x \approx 12\lambda$ (before the interaction the nanofilm was located at point $x \approx 10\lambda$), and the electrons near the axis ($y = 25\lambda$) move synchronously in the direction of the laser pulse propagation. At the same time, away from the axis the electrons begin to turn back because the laser pulse field there decreases according to a Gaussian law. At $t = 4.5T_0$, the electrons at the left boundary of the relativistic electron mirror have already turned back, while the electrons at the right boundary continue to move forward. Finally, at $t = 5.9T_0$, the electrons that first turned back reach the right boundary of the ion layer, where there are ions with maximum energy. Since that time, the field, which accelerates these ions, starts to decrease. Thus, the effective acceleration time t_{ea} is equal to the time of the longitudinal electron return, t_r, and can be roughly estimated as a doubled lifetime of the relativistic electron mirror, $t_l : t_{ea} = t_r \approx 2t_l$. A more accurate estimate can be obtained by taking into account the longitudinal displacement of the ions with maximum energy:

$$\tilde{t}_r = \frac{\sqrt{1 + 8\zeta\tilde{t}_l} - 1}{2\zeta}. \qquad (3)$$

Figure 1 shows the vertical lines that mark specific points in time during the acceleration of the ions. The vertical line with squares corresponds to an estimate of the effective acceleration time by the results of two-dimensional numerical simulation, and the line with diamonds – an assessment from equation (3) with the lifetime of the mirror obtained in the simulation. Also shown is the time when the electrons from the nanofilm periphery compensate for the charge of the ions on the axis due to their transverse motion along the film surface (line with triangles). The lines with squares and diamonds virtually coincide and lie near the inflection point of the acceleration curve, whereas the line with triangles is much more to the right, where any features on an acceleration curve are absent. Thus, in this case, the effective acceleration time is completely determined by the return of electrons located at the left boundary of the relativistic electron mirror.

3.2. Limiting the maximum ion energy due to transverse motion of electrons along the nanofilm surface

The phase spaces x, y of the ions and electrons in the nanofilm ($\alpha = 3$) during their acceleration by a laser pulse with $a_0 = 30$ are shown in Fig. 3 at different points in time from the beginning of interaction. The dynamics of the electron motion is significantly different from that in Fig. 2, because the motion along the surface of the nanofilm is clearly pronounced. Shifting to the centre, the electrons compensate for the charge of positive ions and reduce the accelerating field. As a result, at $t = 12.5T_0$, the electrons close up, and the field amplitude is greatly reduced. Near the axis, the electrons at this time have already turned back, but have not yet reached the right boundary of the ion layer; therefore, their influence on the dynamics of ions is insignificant.

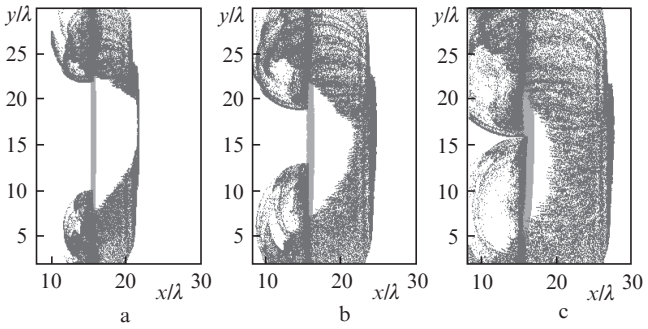

Figure 3. Phase spaces x, y of the electrons (dark grey areas) and the ions (light grey areas) at $t = 6.5T_0$ (a), $9.5T_0$ (b) and $12.5T_0$ (c) from the beginning of interaction. Acceleration is implemented by a laser pulse with $a_0 = 30$ for $\alpha = 3$.

Simple estimates show that the Coulomb field of ions in the nanofilm is proportional to α and is so great that the electrons moving along film gain a relativistic speed for the time that is much smaller than the laser pulse period [17]. In confirmation of this, note the shape of the phase space p_y, y of the electrons (p_y is the momentum projection on the y axis), shown in Fig. 4 at $t = 6.5T_0$ (see also Fig. 3a). In this case, the closing time t_c of the electrons in the nanofilm plane has the form

$$\tilde{t}_c \simeq R_0, \qquad (4)$$

where R_0 is the initial diameter (normalised to the wavelength) of a 'positive window' in the nanofilm from which

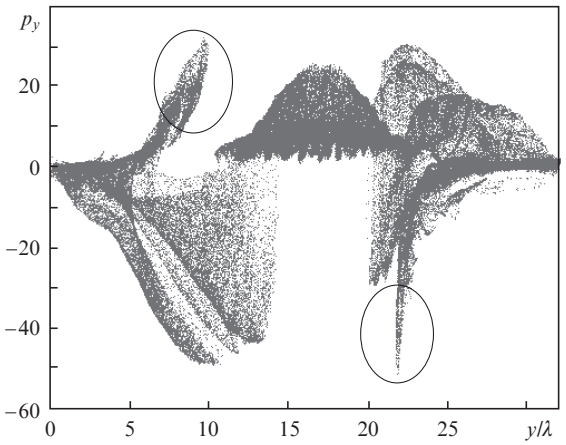

Figure 4. Phase spaces p_y, y of the electrons at $t = 6.5T_0$. The electrons moving along the surface are encircled by ellipses (see Fig. 3a).

electrons are fully evacuated. Given that the evacuation of the electrons is possible if the condition $a_0 > \alpha$ is met [37] (which can also be obtained by comparing the electrostatic and electromagnetic pressures [19, 22]), and the transverse field profile is Gaussian, we obtain an expression for R_0 (the radius of the beam waist w_0 is also normalised to the wavelength)

$$R_0 \simeq w_0 \sqrt{\ln \frac{a_0}{\alpha}}. \tag{5}$$

Analytical estimates of the closing time, obtained from equations (4) and (5) and the data of numerical simulation for different values of w_0 are in good agreement [17].

Figure 5 presents the acceleration curve for the ions with $a_0 = 30$ and $\alpha = 3$. The point in time when the electrons close up is shown by the line with triangles. Estimates of the time of return of the electrons are also given in this figure and the corresponding vertical lines (indicated by squares and diamonds) are located farther from the point of inflection of the acceleration curve than the line for the time of closing of the electrons.

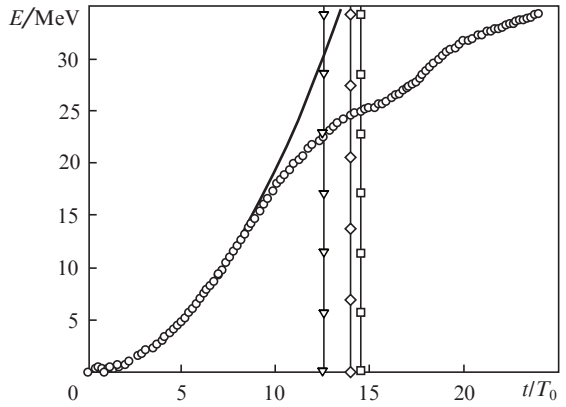

Figure 5. Same as in Fig. 1, but at $a_0 = 30$.

Knowing the dynamics of the transverse motion of electrons upon compensation of the positive ion window, one can improve the estimate of the effective acceleration time compared with its value derived from equations (4) and (5). Indeed, during the time t_c, the ions with maximum energy have time to displace from their equilibrium position (Fig. 3c); therefore, the accelerating field begins to decrease earlier than the positive ion window is completely closed (Fig. 5). To account for this effect, we can introduce the parameter χ using the relation (a_i is the normalised ion acceleration at the right boundary of the nanofilm):

$$R_0 - \tilde{t}_{ea} \simeq \chi S_i \simeq \chi \frac{a_i \tilde{t}_{ea}^2}{2}. \tag{6}$$

This parameter describes the relation between the displacement of the ions with maximum energy from the equilibrium position S_i and size of the positive window $2(R_0 - \tilde{t}_{ea})$ at which the accelerating field decreases (it is assumed that for $\chi = 0$ the field begins to decrease only when the positive window is completely closed; at $\chi = 0.5$, this occurs when the displacement of the ions with maximum energy is equal to the size of the window; and at $\chi = 1$, the displacement is half the size of the positive window). As a result, to improve the estimates of the effective acceleration time, we have the expression

$$\tilde{t}_{ea} = \frac{\sqrt{1 + 4\zeta\chi R_0} - 1}{2\zeta\chi}. \tag{7}$$

Numerical estimates using equations (4) and (5) yield $t_{ea} = 12.16T_0$ and in numerical simulations we obtain an estimate $t_{ea} = 12.5T_0$ (Fig. 3c). From equation (7) we have $t_{ea} = 11.5T_0$ at $\chi = 0.5$ and $t_{ea} = 10.9T_0$ at $\chi = 11$. Judging by Fig. 5, the last two estimates give a better approximation for t_{ea}.

4. Optimisation of the process of ion acceleration by laser pulses with an extremely sharp edge

Based on the above expressions, we can determine the optimal values of the parameters of the laser pulse and nanofilm for effective acceleration. Strictly speaking, optimisation depends on the specific requirements that apply to the ion beam. These can be the requirements to the width of the energy spectrum of ions in the beam, to an angular divergence of the beam, to the total number of ions, etc. In this paper, optimisation is implemented for the maximum ion energy (cut-off energy) as one of the most important parameters which characterises the beam and is easily measured in the experiment.

The energy at the stage of effective acceleration is given by equation (1), where for $\tilde{t}$ it is necessary to use an estimate in accordance with equation (3) or (7). As a result, the maximum energy is determined by $\zeta\tilde{t}_1$, if the energy is limited by the longitudinal return of the electrons of the relativistic electron mirror, or by ζR_0 if the limitation is caused by the transverse motion of the electrons along the nanofilm surface (the parameter χ is assumed constant and specified).

We assume first that the duration of the stage of effective acceleration is limited by the longitudinal return of the electrons (see Figs 1 and 2). For the lifetime of the relativistic electron mirror, use is made of the analytical expression derived in [31]: $\tilde{t}_1 = a_0^2/(8\alpha^2)$. Then, $\zeta\tilde{t}_1 \propto a_0^2/\alpha$, and the maximum energy can be achieved only at the left boundary of the interval for the parameter α, i.e., at constant amplitude of the field a_0, the value of α should be reduced as much as possible. With this decrease, the effective acceleration time increases, and there will come a time when the energy restriction associated with the transverse motion of electrons along the nanofilm surface (Figs 3 and 5) will dominate. Here, $\zeta R_0 \propto \alpha w_0 \times [\ln(a_0/\alpha)]^{1/2}$. The maximum of this expression with respect to α at constant w_0 and a_0 is determined by the equation

$$\alpha_{opt} = \frac{a_0}{\sqrt{e}} = 0.61a_0. \tag{8}$$

As a result, we have

$$\zeta R_0 \propto \frac{a_0 w_0}{\sqrt{2e}} = \frac{1}{\sqrt{2e}} \sqrt{\frac{P}{P_1}}, \tag{9}$$

where P is the laser pulse power; P_1 is the power necessary to produce a field with amplitude $a_0 = 1$ upon focusing to a spot with radius $w_0 = 1$ ($P_1 = 21.6$ GW at $\lambda = 1$ μm for a Gaussian transverse profile).

It follows from expressions (1) and (9) that the maximum ion energy is proportional to laser pulse power P until the ions do not reach relativistic energies, and then growth continues in proportion to $\sqrt{P}$. This dependence is valid if the total acceleration time does not exceed the effective accelera-

tion time, defined by equation (7). At a fixed laser power, the maximum energy is reached if the parameter α is given by (8), and limitation of the acceleration duration – by the time $\tilde{t}_{ea}$ from equation (7), i.e., the condition

$$\frac{\sqrt{1+8\zeta\tilde{t}_l}-1}{2\zeta} = \tilde{t}_t \geqslant \tilde{t}_{ea} = \frac{\sqrt{1+4\zeta\chi R_0}-1}{2\zeta\chi} \qquad (10)$$

should be fulfilled.

For nonrelativistic ion energies or at $\chi = 1$, inequality (10) simplifies and takes the form $2\tilde{t}_l \geqslant R_0$. This inequality should be met only near α_{opt} (8) rather than for arbitrary values of the parameter α, which for the maximum radius of the laser beam waist yields

$$w_0^{max} \leqslant \frac{e}{\sqrt{8}} = 0.961. \qquad (11)$$

This universal relation is valid only for a Gaussian transverse profile of the laser beam; for the super-Gaussian or other profile, condition (11) will be different. Reducing the radius of the waist compared to its optimal value (11) (and a corresponding increase in the amplitude of the accelerating field a_0) does not increase the maximum energy of accelerated ions (in contrast to [13]), but only increases the required value of the parameter α to maintain an optimum acceleration.

The approach developed above makes it possible to optimise the energy of the ions at the time t_{ea}. However, the time itself depends on system parameters, i.e., with changing, for example, the parameter α, t_{ea} also changes. Typically, of interest is the energy of the ions at a certain time t_m. Then, in the general case, the acceleration process will consist of two stages: the effective acceleration of the ions during the time t_{ea}, and then their acceleration during the time $t_m - t_{ea}$ with a decreasing acceleration rate (see Figs 1 and 5). The total energy of the ions will be determined by the sum of the energies accumulated by the ions at each stage. But, because the accelerating pulses have a sharp leading edge and the rate of acceleration at the initial stage is maximal, it is natural to expect that the total energy will be greatest when the energy, accumulated at the stage of effective acceleration is also maximal.

To test this assertion, the above theoretical estimates of the optimal parameters of the system were compared with two-dimensional numerical simulation for two time instants. For definiteness, we used the system parameters $a_0 = 240$ and $w_0 = 1$, i.e., the power of the laser pulse was ~1 PW, which is quite feasible in modern setups. The laser pulse duration was three periods of the field; therefore, one might expect that the radiation reaction effects will not play a significant role [38]. The parameter α changed near the optimum value given by equation (8), from 100 to 140, which corresponds to the target thickness of 100 to 140 nm at the electron density of the order of a solid-state target ($n_0 \approx 320 n_{cr}$). The dependences of the maximum ion energy on the parameter α are given in Fig. 6 for $t_m = 10T_0$ and $50T_0$. The curves exhibit two close local maxima, which is explained by the selected value $w_0 = 1$, somewhat higher than the optimal value (11). The maximum energy in both cases is reached near $\alpha = 135$, which corresponds to $\alpha/a_0 = 0.566$. This value differs from the optimal ratio (8) by less than 10%, i.e., the developed approach can be used to optimise the parameters of the system in a real experiment.

Esirkepov et al. [10] presented the results of two-dimensional multiparametric numerical simulation of ion acceleration by laser pulses. They showed that the maximum ion energy is reached when the ratio

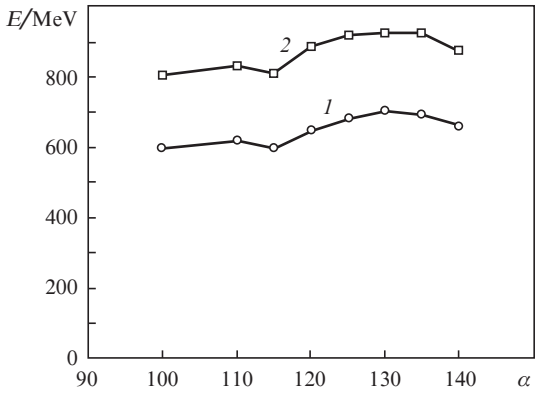

Figure 6. Maximum ion energy as a function of the parameter α for the acceleration time $t_m = 10T_0$ (*1*) and $50T_0$ (2) at $a_0 = 240$ and $w_0 = 1$ (the power is ~1 PW).

$$\frac{n_0 l}{n_{cr}\lambda} \simeq 3 + 0.4a_0 \qquad (12)$$

is fulfilled.

Using expression (8), we obtain the equation:

$$\frac{n_0 l}{n_{cr}\lambda} = (\pi\sqrt{e})^{-1} a_0 \simeq 0.2a_0. \qquad (13)$$

Differences in the optimality conditions (12) and (13) can be explained by significantly different shape and duration of laser pulses used in [10] (a Gaussian pulse with a minimum duration of $10T_0$), and in our paper (a pulse with a rectangular envelope having a duration of $3T_0$). This difference in the pulse duration and shape involves somewhat differing acceleration mechanisms: a mechanism similar to that of TNSA [10] (at least initially), and acceleration by a laser pulse with a sharp leading edge when the electrons are completely displaced at an early stage of interaction (this paper).

The time dependence of the ion energy for the parameter α_{opt} is shown in Fig. 7 [curve (*1*)]. The total acceleration time is $140T_0$, i.e., ~0.5 ps. At the same time, acceleration has the highest rate during the first 10 periods, and the ions gain 90% of the maximum (as shown in Fig. 7) energy during $30T_0$

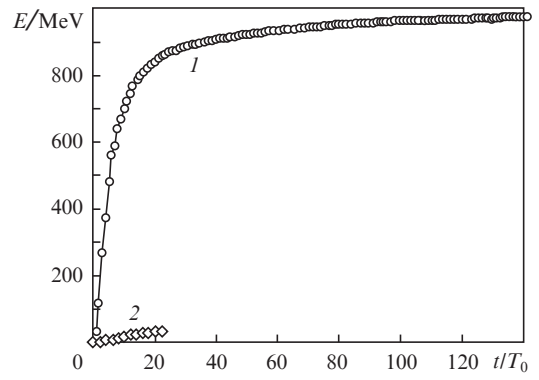

Figure 7. Time dependence of the ion energy at $a_0 = 240$, $w_0 = 1$, $\alpha = 135$ (*1*) and at $a_0 = 30$, $w_0 = 8$, $\alpha = 3$ (*2*).

(~100 fs), after which the time dependence of the energy almost reaches saturation. This behaviour of the ion acceleration is associated with a rather short duration of the accelerating pulse – only three periods of the laser field. As a result, after 20–30 periods most electrons leave the strong laser field region and relax to the equilibrium state. Therefore, we may conclude that the stage of significant charge separation makes the greatest contribution to the maximum energy of the ions. Figure 7 shows, for comparison, the acceleration curve for the same power of the laser pulse, but without optimisation [curve (*2*)] with the parameters $a_0 = 30$, $\alpha = 3$ and $w_0 = 8$, used above for analytical estimates (see Fig. 5). The gain in the maximum ion energy in this case is almost 30 times.

5. Discussion of the results and conclusions

In the above approach, the laser pulse energy does not play an important role. This is due to the fact that we actually consider only the acceleration provided by the steep edge of the pulse during the formation of relativistic electron mirrors and occurring during the time t_{ea}. It is clear that a complete theory should also include the second stage, which is characterised by a decrease in the acceleration rate. In this case, the final energy of the ions after two stages of acceleration will also depend on the laser pulse energy.

Numerical simulation shows that the above-mentioned properties of acceleration are typical not only of laser pulses, for which the amplitude of the first half-cycle is close to the maximum pulse amplitude, but also of the pulses with a Gaussian time profile and a comparable maximum amplitude and energy. This is due to the fact that when the optimisation condition (8) is fulfilled, only the half-cycle with the maximum amplitude can significantly displace the majority of electrons from the equilibrium position and the role of the preceding half-cycles with a smaller amplitude results in the heating of the electrons [31, 34, 37]. As a result, under certain conditions the developed approach can be used in the case of ion acceleration by short laser pulses with a Gaussian shape. A more detailed study of this problem will be presented in subsequent publications.

To verify the obtained analytical results, we used the two-dimensional numerical simulation. Application of the two-dimensional code is fully justified, as long as the displacement of the electrons from the ions does not exceed significantly the size of the focal spot. Such a case is realised for the system parameters used to plot the curves in Figs 1–5. If the above condition is not satisfied, the simulation results may disagree with the experimental data because of the different dependence of the field on the distance for the two- and three-dimensional geometries. In the simulation, whose results are shown in Figs 6 and 7, the diameter of the focal spot was chosen to be 2λ. However, for $\alpha = 100–140$ and the pulse amplitude $a_0 = 240$ used in the simulations, the maximum displacement of the electrons from the ions is less than 2λ, i.e., in this case, the use of the two-dimensional code instead of the three-dimensional code also does not lead to significant errors.

Therefore, we have investigated the processes that limit the maximum energy of the ions during their acceleration by laser pulses with a sharp leading edge. We have evaluated analytically the characteristic parameters of the dynamics of the ions and electrons, allowing optimisation of the laser parameters and nanofilm. When accelerating the ions by short pulses with a Gaussian transverse profile, the maximum ion energy is reached if $\alpha_{opt} = a_0 e^{-1/2}$ upon focusing to a spot of radius $w_0 \lesssim 8^{-1/2}e$. We have shown that the approach makes it possible to significantly increase the final energy of the ions after their acceleration. As a result, when use is made of the laser pulse power of 1–2 TW and energy of 10–20 mJ, protons can be accelerated to energies of 10–15 MeV, and laser systems with a pulse power of ~1 PW and the energy of no more than 10 J allow for laser acceleration of protons up to relativistic energies. Accordingly, 100–300-TW lasers can generate 150–250-MeV ion beams, needed for the practical implementation of hadron therapy of cancer. Such setups are already commercially available, which greatly simplifies their introduction to clinical practice.

Acknowledgements. This work was supported by the Russian Foundation for Basic Research (Grant Nos 09-02-01483-a, 09-02-12322-ofi-m and 11-02-12259-ofi-m-2011) and the Asian Laser Center (APRI GIST, South Korea). H.Suk thanks the National Research Foundation of Korea for financial support under the project Challenge Research Project (Grant No. 2011-0000337).

References

1. Snavely R.A., Key M.H., Hatchett S.P., et al. *Phys. Rev. Lett*., **85**, 2945 (2000).
2. Maksimchuk A., Gu S., Flippo K., et al. *Phys. Rev. Lett*., **84**, 4108 (2000).
3. Andreev A., Levy A., Ceccotti T., et al. *Phys. Rev. Lett*., **101**, 155002 (2008).
4. Henig A., Kiefer D., Markey K., et al. *Phys. Rev. Lett*., **103**, 045002 (2009).
5. Esirkepov T.Zh., Bulanov S.V., Nishihara K., et al. *Phys. Rev. Lett*., **89**, 175003 (2002).
6. Sentoku Y., Cowan T.E., Kemp A., et al. *Phys. Plasmas*, **10**, 2009 (2003).
7. Bulanov S.V., Esirkepov T., Koga J., Tajima T., Farina D. *Fiz. Plazmy*, **30**, 21 (2004) [*Plasma Phys. Rep*., **30**, 18 (2004)].
8. Esirkepov T., Borghesi M., Bulanov S.V., et al. *Phys. Rev. Lett*., **92**, 175003 (2004).
9. Fourkal E., Velchev I., Ma C.-M. *Phys. Rev. E*, **71**, 036412 (2005).
10. Esirkepov T., Yamagiwa M., Tajima T. *Phys. Rev. Lett*., **96**, 105001 (2006).
11. Yin L., Albright B.J., Hegelich B.M., et al. *Laser Part. Beams*, **24**, 291 (2006).
12. Yin L., Albright B.J., Hegelich B.M., et al. *Phys. Plasmas*, **14**, 056706 (2007).
13. Bulanov S.S., Brantov A., Bychenkov V.Yu., et al. *Phys. Rev. E*, **78**, 026412 (2008).
14. Passoni M., Lontano M. *Phys. Rev. Lett*., **101**, 115001 (2008).
15. Brantov A.V., Tikhonchuk V.T., Bychenkov V.Yu., et al. *Phys. Plasmas*, **16**, 043107 (2009).
16. Davis J., Petrov G.M. *Phys. Plasmas*, **16**, 023105 (2009).
17. Kulagin V.V., Cherepenin V.A., Kornienko V.N., et al. *Phys. Lett. A*, **375**, 1135 (2011).
18. Henig A., Steinke S., Schnurer M., et al. *Phys. Rev. Lett*., **103**, 245003 (2009).
19. Macchi A., Cattani F., Liseykina T.V., et al. *Phys. Rev. Lett*., **94**, 165003 (2005).
20. Korzhimanov A.V., Gonoskov A.A., Kim A.V., et al. *Pis'ma Zh. Eksp. Teor. Fiz*., **86**, 662 (2007) [*JETP Lett*., **86**, 577 (2007)].
21. Zhang X., Shen B., Li X., et al. *Phys. Plasmas*, **14**, 073101 (2007).
22. Klimo O., Psikal J., Limpouch J., et al. *Phys. Rev. ST Accel. Beams*, **11**, 031301 (2008).
23. Yan X.Q., Lin C., Sheng Z.M., et al. *Phys. Rev. Lett*., **100**, 135003 (2008).
24. Robinson A.P.L., Zepf M., Kar S., et al. *New J. Phys*., **10**, 013021 (2008).
25. Gonoskov A.A., Korzhimanov A.V., Eremin V.I., et al. *Phys. Rev. Lett*., **102**, 184801 (2009).
26. Qiao B., Zepf M., Borghesi M., et al. *Phys. Rev. Lett*., **102**, 145002 (2009).

27. Schlegel T., Naumova N., Tikhonchuk V.T., et al. *Phys. Plasmas*, **16**, 083103 (2009).
28. Macchi A., Veghini S., Pegoraro F. *Phys. Rev. Lett*., **103**, 085003 (2009).
29. Grech M., Skupin S., Nuter R., et al. *New J. Phys*., **11**, 093035 (2009).
30. Kulagin V.V., Cherepenin V.A., Hur M.S., et al. *Phys. Rev. Lett.*, **99**, 124801 (2007).
31. Kulagin V.V., Cherepenin V.A., Gulyaev Y.V., et al. *Phys. Rev. E*, **80**, 016404 (2009).
32. Nisoli M., De Silvestri S., Svelto O., et al. *Opt. Lett*., **22**, 522 (1997).
33. Tavella F., Nomura Y., Veisz L., et al. *Opt. Lett.*, **32**, 2227 (2007).
34. Kulagin V.V., Cherepenin V.A., Hur M.S., Suk H. *Phys. Plasmas*, **11**, 113102 (2007).
35. Ji L.L., Shen B.F., Zhang X.M., et al. *Phys. Rev. Lett*., **103**, 215005 (2009).
36. Verboncoeur J.P., Langdon A.B., Gladd N.T. *Comput. Phys. Commun*., **87**, 199 (1995).
37. Kulagin V.V., Cherepenin V.A., Hur M.S., Suk H. *Phys. Plasmas*, **11**, 113101 (2007).
38. Chen M., Pukhov A., Yu T.-P., et al. *Plasma Phys. Control. Fusion*, **53**, 014004 (2011).